Indian Journal of Heterocyclic Chemistry
Vol. 28 - Number 03 (Jul-Sep 2018) 345-350

ISSN (Print) : 0971-1627
ISSN (Online) : 2456-4311

Synthesis, Crystal Structure and Properties of 2-Phenyl-1*H*-benzo[d]imidazole-5-sulfonic acid

Lei Guan*, Guanhua Luo, Ying Wang

Department of Inorganic Nometallic Materials, School of Chemistry and Materials Science, Liaoning Shihua University, Fushun 113001, China

ABSTRACT A new UV absorber, 2-phenyl-1*H*-benzo[d]imidazole-5-sulfonic acid (Pbsa), was synthesized, and structurally characterized by single-crystal X-ray diffraction, elemental analysis, IR spectrum, ^{1}H and ^{13}C nuclear magnetic resonance. The product crystallizes in monoclinic system, space group $P2_1/n$ with $a = 9.9475(14)$, $b = 8.8269(12)$, $c = 16.459(2)$ Å, $\beta = 100.620(2)°$, $V = 1420.4(3)$ Å^3, $Z = 4$, and $R_{gt}(F) = 0.0513$, $wR_{ref}(F^2) = 0.1264$. The UV-Vis absorption in the region of 290 and 360 nm is attributed to the conjugated system. The result of biochemical tests can show that Pbsa is not toxic and cannot damage the liver, renal, pancreatic, and ion metabolism functions of the experimental mice through skin and wounds. It can be used for skin sunscreen without acute skin toxicity. It shows the good photostability, which can be comparable to that of commercially available UV absorber, UV1577.

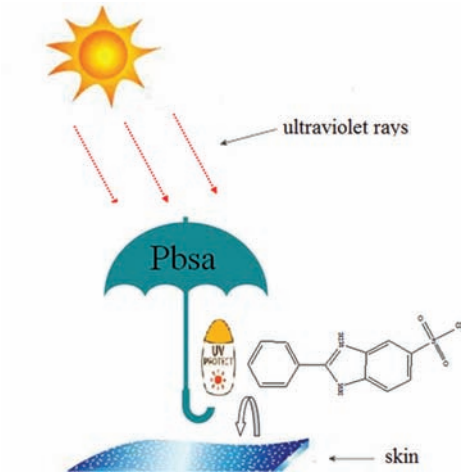

The biochemical test shows that Pbsa can be used for skin sunscreen without acute skin toxicity

KEYWORDS Synthesis, Crystal structure, 2-Phenyl-1*H*-benzo[d]imidazole-5-sulfonic acid, Toxicity.

INTRODUCTION

Ultraviolet protection of organic and biological materials against photodestruction has drawn more attention from researchers. The protection can be realized by use of UV absorbers. UV absorbers are always organic compounds, which can be divided into ketone, acrylonitrile, benzotriazole, etc., according to their chemical structures.[1-3] They can absorb all UV light, and convert light energy into heat, along with their degradation process. The organic UV absorbers are most frequently used in cosmetics and sunscreen to prevent sunburns and skin cancer.[4-6] Furthermore, the textiles modified with organic UV absorbers can play a role in the protection of the skin.[7-9] Multi-nuclear N-heterocyclic compounds like

*Corresponding author: Email: glmater@163.com

Published & Hosted by :

Journal Homepage :
www.connectjournals.com/ijhc

www.connectjournals.com

benzimidazole are an important kind of organic UV absorber and have drawn extensive examinations of many researchers for a long time. They can exhibit excellent absorption of ultraviolet radiation because of their larger conjugated system and substituent groups. The class of compounds is non-toxic, low irritant, and low allergic therefore, they have a wide range of applications, which could be used as the UV absorber in sunscreen and skin care cosmetics. The famous products were reported.[10-12] The synthesis of benzimidazole and its derivatives has been one of the research hotspots.

Recently, the types of sunscreens have emerged in an endless stream; however, the consumers are increasingly questioning the safety of them. The toxicity of UV sunscreen has been paid more and more attention. Therefore, before the sale, the safety evaluation of sunscreens is particularly important. The acute skin toxicity test can examine the effects of sunscreens on the function, physiology, and biochemistry of the whole body and is an indispensable method for evaluating the safety of sunscreens. However, the study on the toxicity of UV sunscreen in China has just started.[13-16]

Here, we report the synthesis, crystal structure and characterization of a new derivative, Pbsa, together with UV-Vis absorption spectrum and photostability analysis. Biochemical tests have also been carried out.

RESULTS AND DISCUSSION

Crystal structure

The molecular structure of Pbsa is shown in **Figure 1**. The selected bond lengths and angles are in the expected ranges. The N-C band lengths are between 1.338 (4) and 1.388 (4) Å, shown in **Table 1**. The whole molecule shows non-mirror symmetry. The asymmetric unit contains one Pbsa and two free water molecules. The hydrogen ion of the sulfonate group in the molecule is dissociated. The nitrogen atom in the molecule is H-protonated. The sum of the valence of the whole molecule is zero. The dihedral angle is 3.02° between benzimidazole plane and benzene plane. It can be said that the conjugated system of this molecule is relatively large. The bond length of C7-C8 is 1.457 (4) Å, which is between the C-C single bond and C-C double bond. Furthermore, the value is larger than other C-C bond lengths in the aromatic ring of this molecule. The bond length of C7-C8 varies with the conjugation effect. It can be proved that benzene and benzimidazole rings have conjugate effects.

UV-Vis absorption property

The UV-Vis spectrum of Pbsa was recorded in the solid state. As illustrated in **Figure 2**, the absorption in the region of 290 and 360 nm is due to π-π transition. From the structural analysis, the introduction of the phenyl group can increase the conjugation system and the maximum absorption wavelength. Therefore, UV absorption property increases obviously. The sulfonate group on the UV absorption property has little effect.[17]

Toxicity test

To investigate the biological properties of the Pbsa sample, the toxicity tests can be carried out. Toxicity tests include liver and renal function, electrolyte, blood glucose, blood lipids, and myocardial enzyme examination contents.

The toxicity tests were performed with the obtained serum samples.[18-20] The statistical results are listed in **Tables 2 and 3.** Alanine aminotransferase (ALT) is identified as the most sensitive indicator of liver function damage by the World Health Organization. In clinical medicine, aspartate aminotransferase (AST), lactate dehydrogenase

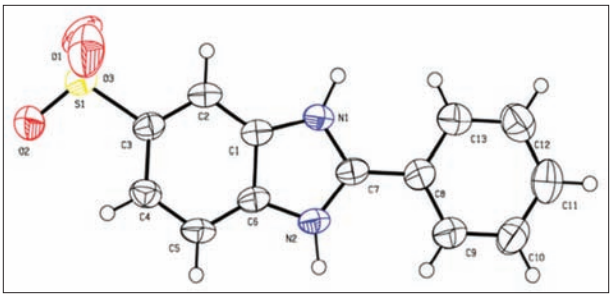

Figure 1: Molecular structure of Pbsa (Two free water molecules are omitted)

Table 1: Selected bond lengths (Å) and bond angles (°)

Bond	Dist.	Bond	Dist.
C1-N1	1.379 (4)	C7-N1	1.342 (4)
C1-C2	1.381 (4)	C7-C8	1.457 (4)
C1-C6	1.397 (4)	C8-C13	1.379 (4)
C2-C3	1.383 (4)	C8-C9	1.390 (4)
C3-C4	1.404 (4)	C9-C10	1.374 (5)
C3-S1	1.774 (3)	C10-C11	1.366 (5)
C4-C5	1.379 (4)	C11-C12	1.377 (5)
C5-C6	1.382 (4)	C12-C13	1.378 (5)
C6-N2	1.388 (4)	O1-S1	1.434 (3)
C7-N2	1.338 (4)	O2-S1	1.431 (2)
O3-S1	1.441 (3)		
Angle	**(°)**	**Angle**	**(°)**
N1-C1-C2	131.7 (3)	C9-C8-C7	120.2 (3)
N1-C1-C6	106.5 (3)	C10-C9-C8	120.3 (3)
C2-C1-C6	121.8 (3)	C2-C3-C4	121.9 (3)
C1-C2-C3	116.5 (3)	C11-C10-C9	120.4 (3)
C2-C3-S1	118.6 (2)	C10-C11-C12	119.8 (4)
C4-C3-S1	119.4 (2)	C11-C12-C13	120.3 (4)
C5-C4-C3	121.2 (3)	C12-C13-C8	120.2 (3)
C4-C5-C6	117.0 (3)	C7-N1-C1	109.5 (2)
C5-C6-N2	132.2 (3)	C7-N2-C6	109.4 (2)
C5-C6-C1	121.7 (3)	O2-S1-O1	113.41 (18)
N2-C6-C1	106.1 (3)	O2-S1-O3	112.03 (18)
N2-C7-N1	108.4 (3)	O1-S1-O3	112.3 (2)
N2-C7-C8	126.0 (3)	O2-S1-C3	107.74 (14)
N1-C7-C8	125.6 (3)	O1-S1-C3	105.55 (15)
C13-C8-C9	118.9 (3)	O3-S1-C3	105.17 (16)
C13-C8-C7	120.8 (3)		

Table 2: Biochemical assay of serum toxicity test after dressing

Group index	Dressing period		Recovery period	
	Blank group/A1-D	Dressing group/A2-D	Blank group/A1-R	Dressing group/A2-R
TP	57.96±4.32	52.71±2.68*	50.77±5.04	55.65±0.64
B	41.06±2.49	35.84±2.37*	33.37±3.93	38.75±1.20
GLOB	16.9±3.38	16.87±1.32	17.40±1.42	16.90±1.84
A/G	2.5±0.49	2.13±0.23	1.90±0.17	2.30±0.28
TBIL	1.75±0.39	2.34±0.97	2.53±0.45	1.50±1.13
ALP	132±55.40	104.71±29.04	65.33±14.84	84.50±14.85
GGT	1.43±1.13	1.57±0.53	0.67±0.58	2.00±1.41
ALT	33.43±6.70	37.43±9.52	40.00±2.65	31.50±0.71
AST	88.71±25.53	107.57±23.59	54.67±39.83	88.50±24.75
AST/ALT	2.65±0.65	2.94±0.65	2.24±0.71	2.80±0.72
CK	726.33±286.49	1023.71±388.17	569.67±400.25	391.50±379.72
TG	2.12±1.10	1.29±0.39	1.02±0.31	1.05±0.07
CHOL	1.94±0.43	1.91±0.24	2.30±0.97	1.55±0.14
K	7.31±0.68	7.42±0.52	6.63±0.45	5.95±0.64
NA	155.57±3.69	153.5±1.87	153.00±2.00	149.50±2.12
CL	106.29±2.43	103.17±2.23*	103.00±2.65	103.50±2.12
OSM	330.93±6.68	331.1±3.64	326.85±3.15	319.54±6.68
UREA	9.2±1.86	8.59±1.07	7.80±0.61	7.70±1.84
CREA	14.71±1.80	8.57±1.27	9.33±3.51	11.00±1.41
Glu	51.71±108.52	9.38±1.03	7.58±0.63	8.64±1.17
EGFR	285.80±17.10	354.92±20.44*	350.83±55.80	319.47±16.92

ALT: Alanine aminotransferase, AST: Aspartate aminotransferase, ALP: Alkaline phosphatase, TBIL: Total bilirubin, CREA: Serum creatinine, UREA: Serum urea, TP: Total serum protein, GGT: Gamma-glutamyltransferase, CHOL: Cholesterol, TG: Triglycerides, CK: Creatine kinase, EGFR: Epidermal growth factor receptor

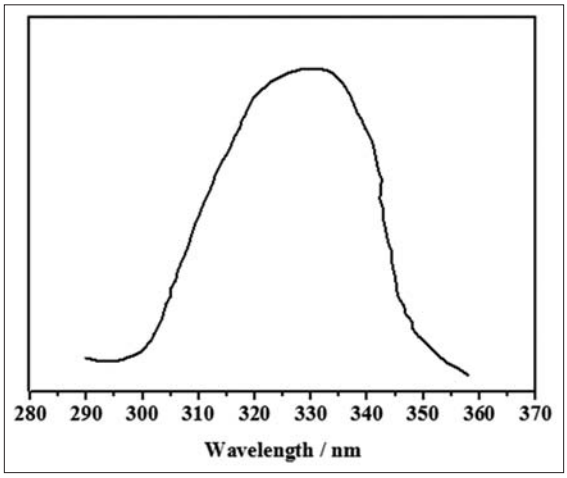

Figure 2: Solid state UV-Vis spectrum of Pbsa at room temperature

(LDH), alkaline phosphatase (ALP), and total bilirubin (TBIL) are the indicators to judge whether the damage to the liver. Serum creatinine (CREA) and serum urea (UREA) are the main indicators of renal function. The abnormities of them mean the damage to renal function. The Glu indicator is used to determine whether the pancreas is damaged. The K, NA, and CL indicators are used to determine whether the metabolism of ions is damaged. Hence, we mainly focus on these indicators to examine the toxicity of Pbsa. The other indicators are used to assist in the decision.

It can be seen that the indicators in A2-D group, such as ALT, AST, LDH, ALP, TBIL, CREA, and UREA, show no significant differences with those of A1-D group. This means that the Pbsa has no damage to the liver and renal functions of the mice. However, in the dressing period, the CL indicator in the A2-D group can show a significant difference with one of the A1-D group. Furthermore, it can return to normal during the recovery period. This result can suggest that Pbsa does not cause damage to the ion metabolic pathways in the mice. The other indicators with the significant differences are similar to the CL indicator, which all can restore to normal in the recovery period.[19,20] It could be said that the significant differences of the indicators could originate from a stress response to Pbsa in mice, and Pbsa does not cause damage or adverse reactions to the mice.

Toxicity tests were also carried out on the wound of mice to ensure that Pbsa was directly exposed to wounds and could not cause damage to mice. The result can be used to determine the absorption of Pbsa directly through muscle tissue, and blood cannot damage the organ function of mice. This is the safety test before Pbsa is applied.

The mice were scratched, and the wounds were directly affected by Pbsa. The indicators of A4-D, such as A/G, TBIL, AST, TG, and K, have significant differences with those of A3-D. However, in addition to the TG indicator, the other indicators with significant differences are all restored to normal during the recovery period. It is worth noting that ALP indicator of A4-D in the dressing period is normal, but in the

Table 3: Biochemical assay of serum of toxicity test in the recovery period

Group index	Dressing period		Recovery period	
	Scratching group/A3-D	Scratching and dressing group/A4-D	Scratching group/A3-R	Scratching and dressing group/A4-R
TP	57.19±3.74	55.49±2.57	53.43±1.40	53.13±3.27
ALB	36.17±3.13	38.56±2.42	38.73±1.76	38.53±0.71
GLOB	21.01±1.31	16.93±1.17	14.70±1.14	15.60±2.00
A/G	1.73±0.16	2.29±0.23*	2.63±0.31	2.50±0.30
TBIL	2.6±0.52	1.66±0.21*	1.35±0.07	1.67±0.15
ALP	72.43±20.91	118.71±29.72	108.00±12.12	71.33±15.30*
GGT	1±0.58	1.43±0.98	0.67±0.58	1.00±0.00
ALT	45.86±18.68	31±4.62	29.67±6.03	35.33±6.66
AST	151.86±48.54	82.43±19.33*	94.00±48.08	81.33±8.08
AST/ALT	3.57±1.38	2.7±0.72	2.82±1.05	2.33±0.25
CK	1574±1082.70	698.71±376.71	569.00±664.68	466.00±127.43
TG	0.80±0.19	1.22±0.45*	1.33±0.10	1.05±0.11*
CHOL	2.34±0.57	2.20±0.58	1.97±0.56	1.34±0.31
K	8.37±1.64	8.87±0.76*	6.07±0.80	6.53±0.21
NA	154.71±3.86	152±1.41	151.00±2.65	151.00±1.00
CL	105.43±3.86	102.86±1.95	104.33±3.51	104.33±0.58
OSM	333.55±9.00	327.02±3.50	322.27±8.12	328.82±2.18
UREA	7.83±1.40	8.36±1.15	8.90±1.23	9.83±1.31
CREA	10.14±1.77	9±1.63	10.67±2.08	11.00±2.00
GLU	7.38±2.15	9.28±1.10	8.37±0.22	8.75±0.24
Egfr	332.34±26.63	348.78±24.70	325.03±24.90	320.78±24.34

ALT: Alanine aminotransferase, AST: Aspartate aminotransferase, ALP: Alkaline phosphatase, TBIL: Total bilirubin, CREA: Serum creatinine, UREA: Serum urea, TP: Total serum protein, GGT: Gamma-glutamyltransferase, CHOL: Cholesterol, TG: Triglycerides, CK: Creatine kinase, EGFR: Epidermal growth factor receptor

recovery period, it has a significant difference with the one in A3-R group. The ALP indicator of A4-R group in the recovery period decreased significantly, compared with the one of A3-R group. The decrease of ALP indicator has no clinical significance and cannot judge the damage of liver function. Moreover, other liver function indicators, including the most sensitive indicator ALT, do not appear to be abnormal, so it is confirmed that the liver function has not been damaged.[13-16] In the dressing period, the K indicator in the A4-D group can show a significant difference, compared with A3-D. However, it returned to normal during the recovery period. This result can suggest that Pbsa does not result in the damage to the ion metabolic pathways of the mice.

The Glu indicators in the A2-D and A4-D groups do not show significant differences compared with the reference groups in the dressing period. Furthermore, in the recovery period, there are no significant differences for this indicator. This means that Pbsa does not damage the function of the pancreas.

The biochemical tests shows that the direct effect of Pbsa on the skin and on the wound cannot result in the functional damage and death of experimental mice. It could be used for skin sunscreen without acute skin toxicity.

Photostability

To investigate the property of photostability of Pbsa, we performed a comparative test with Pbsa and commercially available UV1577. The Pbsa and UV1577 were dissolved in an ethanol-water solvent. The concentration is 2.5×10^{-5} mol/L. The solution can be left in UV light box treating during 10–50 h, respectively. The treated solution was tested with UV-Vis spectra at room temperature. The intensity of the absorption peak varies with different UV exposure time, as shown in **Figure 3**. It can be seen that Pbsa and UV1577 are degraded gradually with the extension of light duration. The photostability of Pbsa is comparable to that of commercially available UV absorber, UV1577, which can show good photostability.[17]

EXPERIMENTAL SECTION

Materials and measurements

All reagents were purchased commercially and used without further purification. The mice (7 weeks old, half of male and female, and weighing 300–400 g), were bought from the biotechnology company. X-ray single crystal diffraction data were collected at 296 K from a single crystal mounted atop a glass fiber with a Bruker Smart CCD diffractometer using graphite-monochromated Mo K_a (λ = 0.71073 Å) radiation. ^{1}H and ^{13}C nuclear magnetic resonance (NMR) spectra were recorded on a Bruker AV 400 spectrometer. The Fourier-transform infrared (FT-IR)

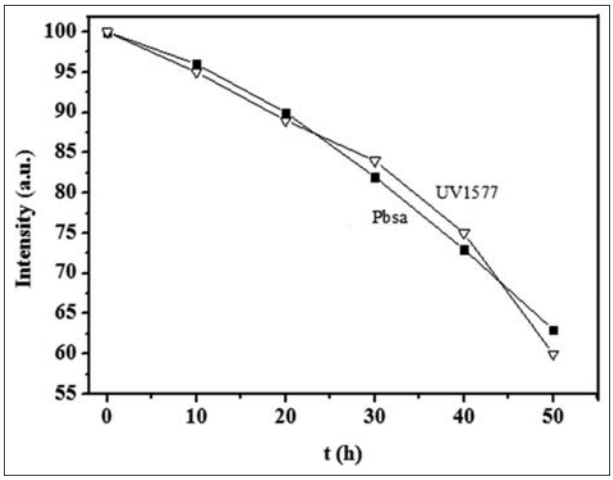

Figure 3: Relative intensities of UV absorption peaks of Pbsa and UV1577 after different UV exposure time

spectrum was recorded on a Nicolette FT-IR spectrometer using KBr pellets in the range of 4000–400/cm. Elemental analysis (C, H and N) was performed on a Perkin-Elmer 240C analyzer. The UV-Vis absorption spectrum was recorded on a TU-1901 spectrophotometer. The toxicity test was carried out using a SCXK-automatic biochemical analyzer.

Synthesis and characterization

3,4-Diaminobenzenesulfonic acid (18.82 g, 0.01 mol) and benzoic acid (12.21 g and 0.01 mol) were dissolved in DMF and water (1:1 v%) solution. Using trimethylsilyl chloride as the catalyst, the mixture was heated in the microwave reactor at 110°C for 0.5 h. After heating, it was adjusted to 10 of pH value. In the end, the precipitation was filtered and separated. The blocked crystal of the product was obtained on recrystallization. After removal of water molecules from the products, the characterizations were measured. **^{1}H-NMR** (dimethyl sulfoxide [DMSO]): 8.28 (d), 7.90 (s), 7.59 (d), 7.51 (d), 7.41 (s), 5 (s) ppm; **^{13}C-NMR** (DMSO): 152.9, 145.5, 140.2, 137.9, 134.7, 131.1, 129.2, 127.5, 120.7, 116.5, 113.2 ppm. **Anal. calcd.** for $C_{13}H_{10}N_2O_3S$ (310.32): C, 50.31; H, 3.22; N, 9.02; S, 10.33; found C, 50.66; H, 3.81; N, 9.25; S, 10.79. **IR spectrum** (cm^{-1}), 3375, 2857, 1632, 1601, 1568, 1514, 1496, 1375, 1212, 1089, 1030, 870, 777, 683, 614.

X-ray crystallographic measurement

Data collection for Pbsa was carried out on a Bruker Smart CCD diffractometer equipped with graphite-monochromated Mo K_α radiation (λ = 0.71073 Å) at 296 K. Data reduction were performed with SAINT, and empirical absorption corrections were applied by the SADABS program. Structures were solved by direct methods using the SHELXS program and refined with the SHELXL program.[21-23] The other non-hydrogen atoms were directly obtained from a difference Fourier map. Final refinements were performed by full-matrix least-squares methods with anisotropic thermal parameters for all non-hydrogen atoms on F^2. C-bonded H atoms were placed geometrically and refined as riding model. Selected bond distances and bond angles are listed in **Table 1**.

Experimental treatment

A total of 48 mice were divided into four groups, including blank group (A1, the reference group), dressing group (A2), scratching group (A3, the reference group), scratching, and dressing group (A4). The mice in A1 and A3 groups were daubed with physiological saline once a day for 30 days (marked as the groups of A1-D and A3-D, respectively), and the mice in A2 and A4 groups were smeared with Pbsa once a day for 30 days (marked as the groups of A2-D and A4-D, respectively). These phases are called dressing period. The mice were taken for blood; then the blood samples were centrifuged to take the serum. The blood-collecting mice continued to be reared for 2 weeks without smearing the physiological saline or Pbsa; these phases are called recovery period (marked as the groups of A1-R, A2-R, A3-R, and A4-R, respectively); subsequently, the blood samples were collected and centrifuged to separate the serum.

After a night of fasting, the blood samples were collected through the veins of the mice. The blood samples (blood volume is about 0.8–1.2 mL) were placed in 1.5 mL centrifuge tubes, and then were centrifuged to separate the serum in the condition of 4℃, 3000 rpm.

Statistical analysis

In the statistical analysis, 12 parallel samples were set in each group, and all the data were finally expressed in the form of average value ± variance. The analysis of variance was carried out by ANOVA method. SPSS software was used to analyze the data. *means a significant difference, compared with the reference ($P \leq 0.01$).

CONCLUSION

A new UV absorber, Pbsa, was synthesized. The benzene and benzimidazole rings in Pbsa molecule have conjugate effects. The UV-Vis absorption in the region of 290 and 360 nm can be attributed to the conjugated system. The biochemical test showed that Pbsa directly affects the skin and on the wound, and did not cause abnormalities in the function of the visceral organs and the death of experimental mice. It can be used for skin sunscreen without acute skin toxicity. Its photostability is similar to that of commercially available UV absorber.

Funding

This work was supported by the Department of Education of Liaoning Province (grant number L2015299).

ACKNOWLEDGMENTS

We are thankful to the doctors in the clinical laboratory, an affiliated hospital of Liaoning University of traditional Chinese medicine.

REFERENCES

[1] Keck, J., Kramer, H.E.A., Port, H., Hirsch, T., Fischer, P., Rytz, G. Investigations on polymeric and monomeric intramolecularly hydrogen-bridged UV absorbers of the benzotriazole and triazine class, *J. Phys. Chem.*, **1996,** *100*, 14468–14475.

[2] Rubí, E., Cela, R. Solid-phase extraction followed by liquid chromatography-tandem mass spectrometry for the determination of hydroxylated benzophenone UV absorbers in environmental water samples, *Anal. Chim. Acta*., **2009**, *654*, 162–170.

[3] Lapidot, N., Gans, O., Biagini, F. Advanced Sunscreens: UV Absorbers Encapsulated In Sol-Gel Glass Mmicrocapsules, *J. Sol-Gel Sci. Tech.*, **2003**, *26*, 67–72.

[4] Rottman, C., Gans, O., Biagini, F. Sol-gel products news: Advanced sunscreens: UV absorbers entrapped in sol-gel glass microcapsules, *J. Sol-Gel Sci. Tech*., **2002**, *23*, 268–270.

[5] Schaller, C., Rogez, D., Braig, A. Hydroxyphenyl-s-triazines: Advanced multipurpose UV-absorbers for coatings, *J. Coatings Technol. Res.*, **2008**, *5*, 25–31.

[6] Herzog, B., Wehrle, M., Quass, K. Photostability of UV absorber systems in sunscreens, *Photochem. Photobiol.*, **2009**, *85*, 869–878.

[7] Tang, E., Cheng, G., Ma, X., Pang, X., Zhao, Q. Surface modification of zinc oxide nanoparticle by PMAA and its dispersion in aqueous system. *Appl. Surf. Sci.*, **2006**, *252*, 5227–5232.

[8] Yadav, A., Prasad, V., Kathe, A.A., Raj, S., Yadav, D., Sundaramoorthy, C., Vigneshwaran, N. Functional finishing in cotton fabrics using zinc oxide nanoparticles, *Bull. Mater. Sci.*, **2006**, *29*, 641–645.

[9] Vigneshwaran, N., Kumar, S., Kathe, A.A., Varadarajan, P.V., Prasad, V. Functional finishing of cotton fabrics using zinc oxide-soluble starch nanocomposites, *Nanotechnology*, **2006**, *17*, 5087–5095.

[10] Xin, J.H., Daoud, W.A., Kong, Y.Y. A new approach to UV-blocking treatment for cotton fabrics, *Text. Res. J.*, **2004**, *74*, 97–100.

[11] Mahltig, B., Böttcher, H., Rauch, K., Dieckmann, U., Nitsche, R., Fritz, T. Optimized UV protecting coatings by combination of organic and inorganic UV absorbers, *Thin Solid Films*, *2005*, *485*, 108–114.

[12] Pollack, J.B., Ragent, B., Boese, R., Tomasko, M.G., Blamont, J., Knollenberg, R.G., Esposito, L.W., Stewart, A.I., Travis, L. Nature of the ultraviolet absorber in the venus clouds: Inferences based on pioneer venus data. *Science*, **1979**, *205*, 76–79.

[13] Gago-Ferrero, P., Díaz-Cruz, M.S., Barceló, D. An overview of UV-absorbing compounds [organic UV filters] in aquatic biota, *Anal. Bioanal. Chem.*, **2012**, *404*, 2597–2610.

[14] Hayden, C.G., Cross, S.E., Anderson, C., Saunders, N.A., Roberts, M.S. Sunscreen penetration of human skin and related keratinocyte toxicity after topical application, *Skin Pharmacol. Phys.*, **2005**, *18*, 170–174.

[15] Rodil, R., Moeder, M., Altenburger, R., Schmittjansen, M. Photostability and phytotoxicity of selected sunscreen agents and their degradation mixtures in water, *Anal Bioanal Chem.*, **2009**, *395*,1513–1524.

[16] Foltête, A.S., Masfaraud, J.F., Bigorgne, E., Nahmani, J., Chaurand, P., Botta, C., Labille, J., Rose, J., Férard, J.F., Cotelle, S. Environmental impact of sunscreen nanomaterials: Ecotoxicity and genotoxicity of altered TiO_2 nanocomposites on *Vicia faba*. *Environ. Pollut.*, **2011**, *159*, 2515–2522.

[17] Liu, E.D., Shao, Y.C., Zhang, S.F., Li, X., Qu, L. Synthesis and properties of s-triazine UV absorbents, *Petrochem. Technol.*, **2011**, *40*, 874–878.

[18] Zhang, R., Niu, Y.J., Li, Y.W., Zhao, C.F., Song, B., Li, Y., Zhou, Y.K. Acute toxicity study of the interaction between titanium dioxide nanoparticles and lead acetate in mice, *Environ. Toxicol. Pharm.*, **2010**, *30*, 52–60.

[19] Zou, X.Y., Xu, B., Yu, C.P., Zhang, H.W. Combined toxicity of ferroferric oxide nanoparticles and arsenic to the ciliated protozoa *Tetrahymena pyriformis*. *Aquat. Toxicol.*, **2013**, *134*, 66–73.

[20] Patrick, K., Jemba, J. Excretion and ecotoxicity of pharmaceutical and personal care products in the environment. *Ecotoxicol. Environ. Safe*, **2006**, *63*, 113–130.

[21] Sheldrick, G.M. *SHELXS-97: Program for the Solution of Crystal Structures*, University of Göttingen, Germany, **1997**.

[22] Sheldrick, G.M. A short history of SHELX. *Acta Crystallogr*., **2008**, *A64*, 112–122.

[23] Bruker. *APEX2, SAINT and SADABS*. Brucker AXS Inc., Madison, WI, USA, **2013**.

Received: 26 Apr 2018; Accepted: 04 Jun 2018